Online-Journals.org

iJIM International Journal of Interactive Mobile Technologies

iJIM | eISSN: 1865-7923 | Vol. 19 No. 13 (2025) | OPEN ACCESS

https://doi.org/10.3991/ijim.v19i13.56593

PAPER

Dynamic Adjustment of Mobile Ocean Freight Rates Based on Big Data

Xinning Kang (✉)

School of Economics and Management, Shanghai Maritime University, Shanghai, China

xinningkang2004@163.com

ABSTRACT

Amidst the intensifying competition in the shipping industry and the ongoing digitalization of global trade, ocean freight rates—characterized as multivariate time series—are influenced by a complex interplay of factors including port network structures, market supply and demand dynamics, and transportation costs. Traditional static pricing strategies have proven inadequate in adapting to the rapidly evolving market conditions. Accurate freight rate forecasting has emerged as a critical prerequisite for enabling dynamic adjustment strategies. However, conventional time series models often fail to capture the spatial correlations among multiple entities. Existing graph neural network (GNN)-based approaches typically rely on either predefined static or dynamic graphs, which lack the capacity to effectively model the interactions between inherent static structures and evolving temporal dependencies in the time series data. In this study, the prediction of mobile ocean freight rates was investigated. The intrinsic data characteristics were first analyzed to uncover the coupling mechanism between static structural features and dynamic temporal patterns in time series. A GNN model based on multivariate time series was then proposed to automatically extract dependencies from both static and dynamic graphs through a data-driven graph learning module. An information interaction mechanism was designed to achieve deep fusion of the two types of graph structures, thereby addressing the subjectivity associated with manually defined graphs and the limitations of single-graph modeling approaches.

KEYWORDS

mobile ocean freight rates, dynamic adjustment strategy, graph neural network (GNN), multivariate time series, big data

1 INTRODUCTION

Amid the accelerating integration of global trade and the rapid advancement of shipping digitalization, maritime transport has remained the primary mode of international trade [1, 2], accounting for more than half of global cargo movement.

Kang, X. (2025). Dynamic Adjustment of Mobile Ocean Freight Rates Based on Big Data. *International Journal of Interactive Mobile Technologies (iJIM)*, 19(13), pp. 96–110. https://doi.org/10.3991/ijim.v19i13.56593

Article submitted 2025-03-24. Revision uploaded 2025-05-04. Final acceptance 2025-05-13.

As competition within the shipping market intensifies and supply–demand dynamics grow increasingly volatile [3–5], traditional static freight rate strategies—historically determined through experience—have become insufficient for responding to the real-time fluctuations of modern markets [6, 7]. The proliferation of mobile Internet and Internet of things (IoT) technologies [8, 9] has enabled the real-time acquisition and storage of vast data sources such as port throughput, vessel trajectories, live cargo order volumes, and competitor pricing, laying the data foundation for dynamic freight rate adjustment strategies in the maritime industry [10]. Ocean freight rates, regarded as typical multivariate time series, are subject to the combined influence of numerous interrelated factors, including port network topology, market supply and demand, and transportation costs [11, 12]. A key challenge in the digital transformation of maritime logistics lies in accurately identifying both the inherent static relationships and real-time dynamic disturbances embedded within complex sequential data.

Conventional forecasting approaches for ocean freight rates primarily employ traditional time series models such as autoregressive integrated moving average (ARIMA) and support vector machine (SVM) [13–16]. Although such models are capable of capturing the temporal dependencies of individual variables, they often fail to represent the spatial correlations among heterogeneous entities such as ports, shipping routes, and cargo categories. Consequently, the complex network interactions across nodes within the maritime system are largely overlooked. Recently, emerging graph neural network (GNN)-based models [17, 18] have demonstrated potential in capturing spatial dependencies by constructing port or route relation graphs. However, most existing studies utilize either predefined static or dynamic graphs in isolation, lacking the capacity to jointly model the interactions between static structural patterns and dynamic temporal variations in the time series data.

This study addresses the central question of how data-driven methods can enable accurate forecasting and dynamic adjustment of mobile ocean freight rates. Two key areas were investigated: first, the data characteristics of mobile ocean freight rates were analyzed to explore the static structural features (e.g., hierarchical structures of port networks and long-term cargo flow distributions) and dynamic temporal features (e.g., real-time supply–demand fluctuations and impacts of unexpected events), thereby providing theoretical support at the data level for model development. Second, a forecasting model for mobile ocean freight rates was introduced, in which a GNN-based model for multivariate time series was proposed. A data-driven graph learning module was designed to automatically capture dependencies from both static and dynamic graphs. Furthermore, an information interaction mechanism was incorporated to enable deep integration of the two graph structures, effectively addressing the subjectivity of manually defined graphs and the limitations associated with single-graph modeling approaches.

2 DATA CHARACTERIZATION FOR MOBILE OCEAN FREIGHT RATE FORECASTING

The data used for mobile ocean freight rate forecasting were derived from real-time acquisition and historical accumulation across multiple entities and dimensions within the maritime supply chain, resulting in a multivariate time series

dataset designed to serve as input for the GNN model. From the perspective of participating entities, the data encompass a wide array of sources, including port operators, shipping companies, cargo owners, freight forwarders, regulatory agencies, and third-party platforms. In terms of data types, both static foundational attributes (such as port geographic coordinates, fixed shipping route distances, vessel deadweight tonnage, and other data that remain unchanged or slowly change over the long term) and dynamic real-time signals (such as daily vessel queue durations generated by port congestion alert systems, typhoon trajectory probabilities obtained via satellite remote sensing, and real-time booking records captured on block chain platforms). These data streams have been aggregated in real time through various technologies, including IoT sensors, application programming interfaces (APIs) of enterprise information systems, satellite remote sensing, and web crawlers. They are further integrated with historically archived maritime datasets to form a spatio-temporally coupled database. This multi-source data foundation supports the construction of both static and dynamic graph structures, ensuring that GNN is capable of learning complex dependencies within the maritime system from a data-driven perspective.

As input to the GNN model, the time series data used for mobile ocean freight rate forecasting exhibit a deep interweaving of static structural and dynamic temporal characteristics. From a static perspective, the data reflect stable patterns such as port hierarchy configurations, fixed route networks, and long-term cargo flow distributions. For instance, the geographic layout of hub and feeder ports, annual average cargo volumes on major routes, and long-term capacity allocation agreements between shipping companies and cargo owners constitute a relatively stable network backbone. These features are well-suited for modeling via static graphs to represent inherent dependencies among nodes. From a dynamic perspective, high-frequency variables such as real-time cargo order volumes, fluctuations in fuel prices, port congestion indices, and abrupt changes in international trade policies are present. Examples include capacity reallocation due to congestion in the Suez Canal during a given period or operational efficiency fluctuations at ports caused by typhoon events. These dynamic features form evolving relational networks across different temporal slices and necessitate the use of dynamic graphs to capture real-time node interactions. Together, the static and dynamic features form the composite input to the forecasting model. This includes both low-frequency data that reflect long-term structural regularities within the maritime network and high-frequency signals that capture short-term market disturbances. To accurately learn both the stable structures of static graphs and the temporal dependencies of dynamic graphs, a data-driven graph learning module is required. This approach addresses the limitations of traditional models, which rely on a single graph structure and are thus insufficient for capturing the full complexity of maritime system dependencies.

3 INTRODUCTION OF THE MOBILE OCEAN FREIGHT RATE FORECASTING MODEL

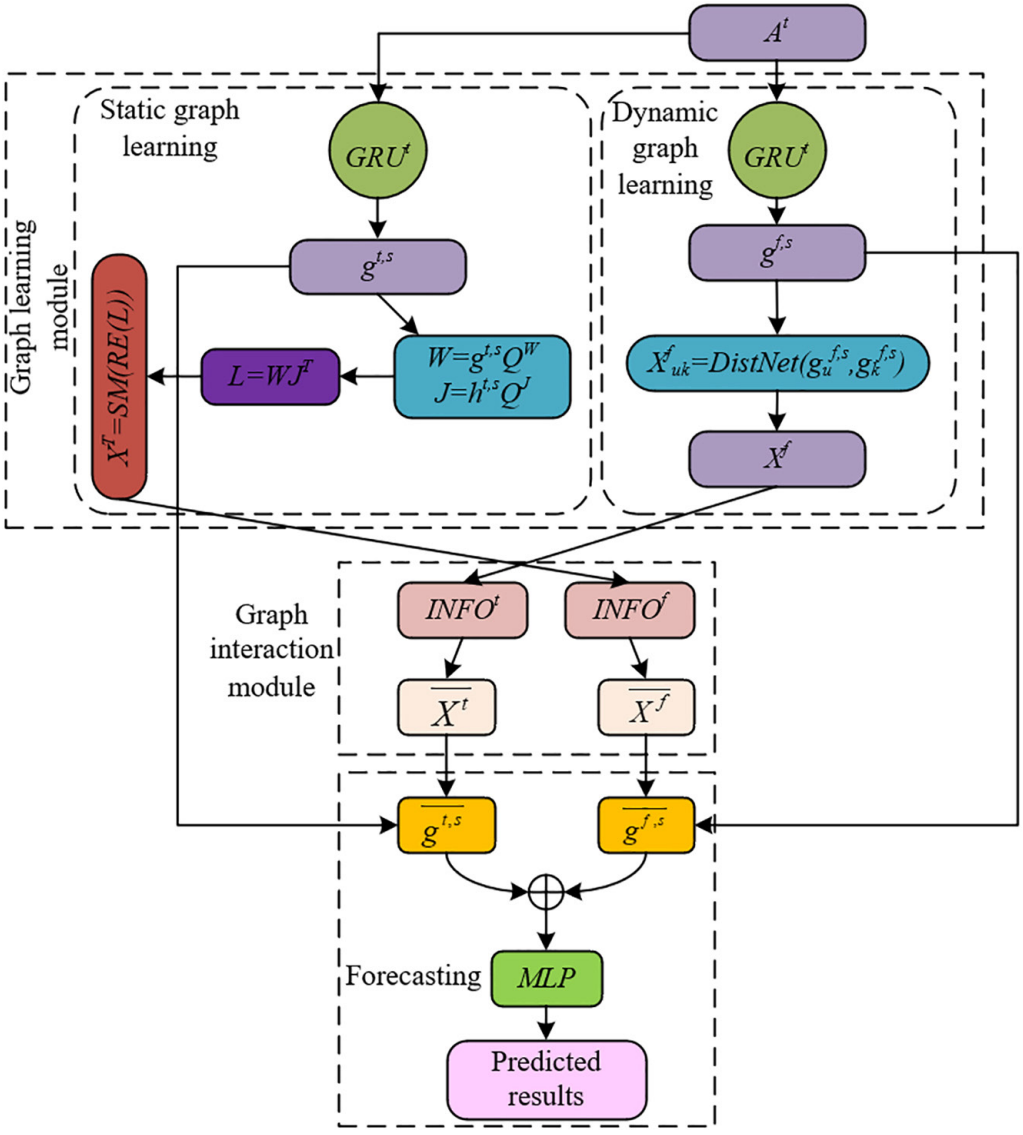

Fig. 1. Overall framework of the mobile ocean freight rate forecasting model

The GNN model constructed for this study was designed to address two core challenges arising from the complex characteristics of the maritime domain. First, static relationships embedded in maritime time series data—such as hierarchical port network structures and baseline capacities of fixed shipping routes—are deeply intertwined with dynamic factors, including real-time cargo volume fluctuations, abrupt fuel price changes, and anomalies in port operations. Traditional methods that rely on manually predefined static graphs or the exclusive use of dynamic graphs for short-term data have proven inadequate in capturing the coupled effects between structural stability and real-time disturbances. To address this limitation, a data-driven graph learning module was incorporated to automatically extract both long-term connections represented by the static graph and instantaneous dependencies captured by the dynamic graph, using heterogeneous data sources such as port throughput, vessel trajectories, and historical freight rates. This approach avoids the omission of

latent relationships that may arise when graphs are manually constructed, such as the unique requirements of refrigerated cargo transport at specific ports or the temporary restructuring of shipping routes due to emergent policy changes. Second, the formation of ocean freight rates is governed by the interaction between static network architectures and dynamic market signals. Traditional models tend to process these two types of information in isolation, resulting in inefficient integration. To overcome this, an efficient information interaction mechanism was implemented. For example, graph convolutional operations were used to extract spatial structural features from static graphs and to capture spatiotemporal evolution patterns from dynamic graphs. These features were then deeply fused through gated integration or feature concatenation strategies. Such fusion allows the long-term influence of hub ports and the short-term impact of sudden cargo overflows to be jointly considered in the forecasting process, thereby mitigating the lag or bias commonly introduced by conventional methods that treat static and dynamic information separately. The overall framework of the proposed mobile ocean freight rate forecasting model is illustrated in Figure 1.

The GNN model constructed for mobile ocean freight rate forecasting was designed to operate on a multivariate time series data matrix $A^t = [A_1^s, A_2^s, \ldots\ldots, A_V^s]$, where V denotes the number of transportation node pairs in the maritime context, M represents the length of the historical observation window, and I includes multiple dimensions of features such as port throughput, fuel prices, vessel capacity, and shipper demand. A dual-graph structure was constructed through a data-driven graph learning module. The static graph defines ports and shipping routes as nodes, with edge weights dynamically generated based on long-term historical cargo flow data to characterize stable connections within the maritime network. The dynamic graph, constructed at the granularity of discrete time slices, embeds real-time variables such as freight rate fluctuations and port congestion indices into node features. Instantaneous dependencies among nodes were then computed using an attention mechanism. Within the graph interaction module, spatial structural features were extracted from the static graph using graph convolutional operations, while spatiotemporal evolution features were simultaneously learned from the dynamic graph. These features were concatenated and subsequently passed through a multilayer perceptron (MLP) to enable both single-step and multi-step freight rate forecasting. The schematic representation of the dynamic graph relationships is illustrated in Figure 2.

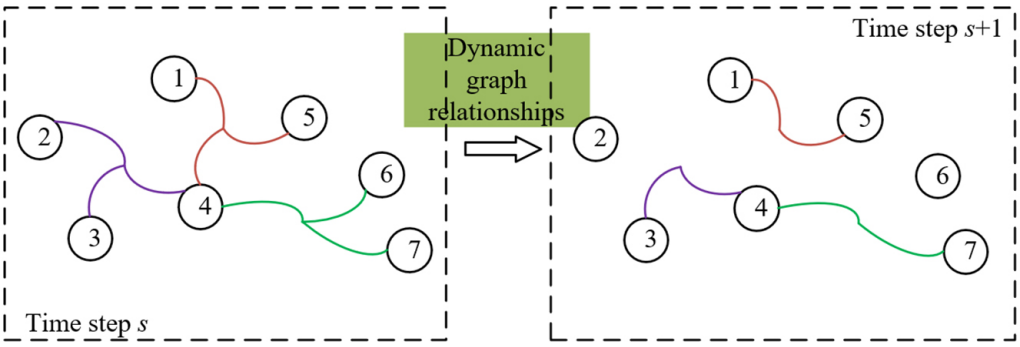

Fig. 2. Schematic representation of dynamic graph relationships

Within the model architecture, a graph learning module was implemented, in which a single-layer gated recurrent unit (GRU) was employed to encode historical time series data. GRU^d and GRU^t with differentiated design were respectively designed for extracting features from both dynamic and static graphs, enabling precise modeling of the dynamic temporal signals and static structural patterns inherent

in maritime freight data. For dynamic graph learning, GRU^d receives high-frequency real-time maritime data as input. Through the coordinated operation of the update gate and reset gate, short-term temporal dependencies related to market disruptions can be dynamically captured. For example, in the event of a sudden port strike that leads to cargo overflow, the update gate in GRU^d increases the weight of the anomalous signal at the current time step, while the reset gate reduces the influence of historically stable conditions. As a result, a dynamic feature representation $g_u^{f,s}$ is generated, which encodes sensitivity to real-time disturbances and serves as temporal input for the adaptive adjustment of edge weights in the dynamic graph. For static graph learning, GRU^t focuses on low-frequency, long-term structural data. By maintaining a relatively high reset gate weight, GRU^t incrementally accumulates stable patterns from historical records, mitigating the risk of excessive forgetting of long-term dependencies. For instance, persistent hub port effects—such as the sustained radiative influence of the Port of Rotterdam in Europe—or baseline seasonal capacity fluctuations along the Asia-Europe shipping corridor are encoded as static features $g_u^{t,s}$, thereby preserving the structural backbone of the maritime network in the static graph. Assuming that the GRUs are denoted by GRU^f and GRU^t, both are used to extract features from A_u^s, which are then used as inputs for the dynamic and static graphs, respectively. The hidden states of the input sequence A_u^s are represented by $g_u^{f,s}$ and $g_u^{t,s}$, corresponding to the dynamic graph f and the static graph t, respectively, and I_g represents the number of hidden units. The corresponding formulas are as follows:

$$g_u^{f,s} = GRU^f(g_u^{f,s-1}, a_u^s) \tag{1}$$

$$g_u^{t,s} = GRU^s(g_u^{T,s-1}, a_u^s) \tag{2}$$

To address the limitations posed by the lack of prior knowledge in maritime networks and the inability of traditional predefined graph structures to capture complex latent dependencies, a static graph learning process was incorporated into the graph learning module. Specifically, a data-driven attention mechanism was employed to automatically infer the adjacency matrix X^t of the static graph, thereby modeling long-term stable dependencies among nodes such as ports and shipping routes. This process begins by feeding historical maritime freight rate time series data into the model. Through global correlation modeling via the attention mechanism, the temporal dependency strength between each node pair over long historical periods was learned. As a result, an adjacency matrix X^t was generated to reflect latent static correlations. Let $g^{t,s} = [g_1^{t,s}, \ldots\ldots, g_V^{t,s}]^T$. Learnable parameters are denoted as Q^W and Q^J, with *Query* and *Key* in the attention mechanism represented by W and J, respectively. The static graph adjacency matrix X^t is expressed as:

$$W = g^{t,s}\, Q^W \tag{3}$$

$$J = g^{t,s}\, Q^J \tag{4}$$

$$L = WJ^T \tag{5}$$

$$X^t = \mathrm{softmax}(\mathrm{ReLU}(L)) \tag{6}$$

To ensure that the learned graph structure exhibits both smoothness and sparsity, a graph regularization term was introduced into the loss function. This term constrains the consistency between feature similarity and adjacency weights across node pairs, guiding the learning process to focus on stable core relationships within

the maritime network while suppressing unnecessary connections between peripheral ports. In doing so, the static graph is enabled to accurately capture the inherent structural dependencies of the ocean freight market. Given the inputs $g_u^{f,s}$ and $g_u^{t,s}$, the graph regularization term is formulated as:

$$M_{HE} = \sum_{u,k=1}^{V} \left\| g_u^{t,s} - g_k^{t,s} \right\|_2^2 X^T + \varepsilon \left\| X^T \right\|_D^2 \tag{7}$$

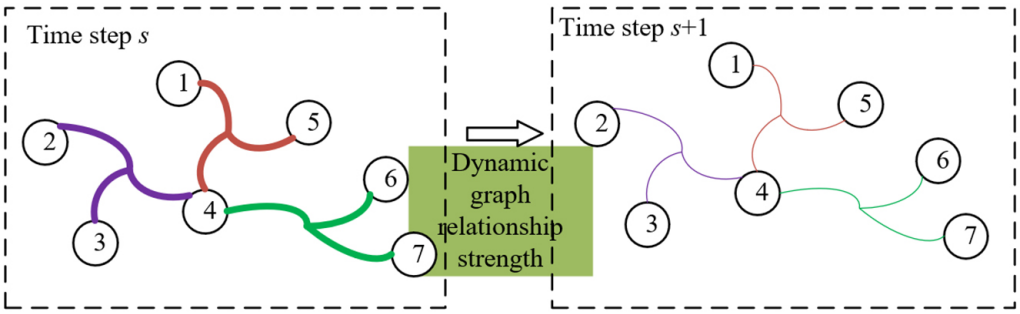

Fig. 3. Schematic of dynamic graph relationship strength

To address the inability of the static graph X^t to model temporal dependencies across time steps, a dynamic graph learning mechanism was incorporated into the graph learning module. This mechanism is based on the temporal hidden states $g_u^{f,s}$ of node samples in the maritime network. By computing a dynamic association strength matrix X^f between temporal samples at different time points, short-term temporal dependencies evolving over time can be effectively captured. A schematic illustration of the dynamic relationship strength is provided in Figure 3. Specifically, the dynamic hidden states $g_u^{f,s}$ were taken as input, and a time-sensitive attention mechanism or dynamic interaction function was employed to quantify the inter-node relational strength across different time steps. The dynamic association weights Xf were adaptively adjusted with each temporal step, allowing the model to reflect evolving dependencies caused by short-term supply–demand fluctuations, sudden disruptions, and policy interventions within the maritime market. Let $\|\cdot\|$ denote the Euclidean norm and *DistNet* (.) denote the distance network. The association strength between $g_u^{f,s}$ and $g_k^{f,s}$ is defined as X_{uk}^f, and can be expressed as:

$$X_{uk}^f = DistNet(g_u^{f,s}, g_k^{f,s}) = \frac{g_u^{f,s} \cdot g_k^{f,s}}{\left\| g_u^{f,s} \right\| \cdot \left\| g_k^{f,s} \right\|} \tag{8}$$

The core objective of the graph interaction module is to achieve complementary information fusion between the static graph and the dynamic graph. Its design is based on the principle of priority to important neighbors, ensuring that key nodes within the maritime network dominate the information aggregation process. In the static graph X^t, edge weights reflect long-term stable cargo flow dependencies between ports, whereas in the dynamic graph X^f, edge weights capture transient associations driven by real-time market signals. An attention mechanism was used to perform weighted selection of neighboring nodes. For a given target port node u, the feature aggregation weights during future freight rate prediction are adjusted based on the real-time importance of each neighboring node k as determined by the dynamic graph X^f. Nodes exhibiting stronger short-term influence contribute more significantly to the aggregation process. Assuming that the output of function *WHERE* (Z, 1, 0) is a vector, if an element Z_u in vector Z is greater than 0, the corresponding element in the

output vector is set to 1; otherwise, it is set to 0. The function *TOPK* (.) returns a vector composed of the top *j* largest values from its input vector, while *MIN* (.) returns a vector consisting of the smallest value(s) in its input vector. The element-wise product is denoted by *p* accordingly, the following expressions are obtained:

$$INFO_{uk}^{t} = \text{softmax}(X_{u}^{f}) = \frac{\exp(X_{uk}^{f})}{\sum_{k=0}^{V} X_{uk}^{f}} \tag{9}$$

$$INFO_{u}^{f} = WHERE(X_{u}^{f} - MIN(TOPK(X_{u}^{t})),1,0) \tag{10}$$

$$\overline{X^{t}} = X^{t} \otimes INFO^{t} \tag{11}$$

$$\overline{X^{f}} = X^{f} \otimes INFO^{f} \tag{12}$$

Given the maritime network's characteristic of structural stability with localized dynamics, the graph interaction module adjusts the edge weights in the static graph X^t in real time through the dynamic graph X^f, incorporating time-varying information without altering the underlying port network structure. Specifically, the row vectors of the dynamic graph adjacency matrix X^f are normalized using the softmax function to obtain the dynamic correlation coefficients (CORR) between each node and all its neighboring nodes. These coefficients reflect the instantaneous dependency strength of node *u* on node *k* at time step *s*. If the dynamic CORR falls below a predefined threshold, the corresponding edge (*u*-*k*) weight in the static graph is attenuated; otherwise, it is reinforced. To prevent excessive model complexity caused by the dynamic graph overfitting to noisy associations, a static graph-guided top-*j* neighbor selection strategy was introduced, ensuring that the dynamic graph retains only the most critical real-time connections for freight rate prediction. Specifically, based on structural metrics such as degree centrality and betweeness centrality in the static graph X^t, the top *j* most important neighbors for each node were first selected. Then, in the dynamic graph X^f, only the connections with these top *j* neighbors were preserved. The edge weights were dynamically adjusted according to real-time data, and ineffective connections with less relevant nodes were removed.

In the context of mobile ocean freight rate forecasting, spatiotemporal feature fusion and information propagation were optimized through graph convolution operations. Static graph features $g^{t,s}$ and dynamic graph features $g^{f,s}$ were first individually convolved with their respective adjacency matrices, resulting in aggregated feature representations $\overline{X^t} g^{t,s}$ and $\overline{X^f} g^{f,s}$, which incorporate information from neighboring nodes. To prevent the loss of intrinsic node characteristics during information propagation, a residual connection mechanism was applied. The original features $g^{t,s}$ and $g^{f,s}$ were added to their respective convolution outputs, yielding enhanced representations. Let the outputs of GRU^t and GRU^f be denoted by $g^{t,s}$ and $g^{f,s}$, respectively. Let α_1 and α_2 represent hyperparameters, Q_1 and Q_2 denote learnable parameters, and y_1 and y_2 denote learnable biases. The convolutional operations can be expressed as:

$$\overline{g^{t,s}} = Q_1 \left(\alpha_1 g^{t,s} + (1-\alpha_1) \overline{X^t} g^{t,s} \right) + y_1 \tag{13}$$

$$\overline{g^{f,s}} = Q_1 \left(\alpha_2 g^{f,s} + (1-\alpha_2) \overline{X^f} g^{f,s} \right) + y_2 \tag{14}$$

During the temporal prediction phase, the enhanced static and dynamic features were concatenated along the temporal dimension, forming a unified feature vector

that incorporates multi-scale spatiotemporal information. This vector was then fed into a two-layer MLP network for prediction. This concatenation strategy facilitates the integration of market signals across different time granularities. The hidden layers of the MLP extract complex feature interactions through nonlinear transformations, while the output layer directly maps to the target prediction values. Let Q_1' and Q_2' denote the learnable parameters of the fully connected layers of the MLP, and let y_1' and y_2' denote the learnable biases. If the dimension of output $\hat{B}$ is represented by v, the computation is expressed as:

$$\hat{B} = \left(\mathrm{ReLU}\left(\left[\overline{g^f}; \overline{g^t} \right] Q_1' + y_1' \right) \right) Q_2' + y_2' \tag{15}$$

Model training was conducted using a multi-objective loss function, which integrates prediction error with graph regularization loss (M_{HE}), thereby achieving a joint optimization of forecasting performance and structural quality of the graph. The graph regularization term constrains the smoothness and sparsity of the adjacency matrix, forcing the model to learn meaningful node associations. Let η denote the hyper parameter. The loss function is expressed as:

$$M_{LO} = \eta M_{HE} + \sum_{u=1}^{m} \left| B_u - \hat{B}_u \right| \tag{16}$$

Following the completion of time series forecasting for mobile ocean freight rates, a dynamic adjustment strategy was used to construct a hierarchical response system based on the predicted results by accounting for the time sensitivity of the maritime market and the decision-making granularity requirements. For short-term predicted freight rates derived from single-step forecasts—such as rates for the next day or the following week—the strategy emphasizes real-time response to immediate market disruptions. For example, if the dynamic graph detects a sudden port strike resulting in a sharp increase in cargo flow, the model's predicted short-term freight surge triggers an immediate pricing module. A dynamic premium mechanism is then activated to rapidly adjust quotations on the affected routes, thereby mitigating short-term supply–demand imbalances and maximizing short-term profitability. For medium- to long-term freight rate sequences generated from multi-step forecasts, the strategy incorporates the structural stability captured by the static graph to guide periodic adjustment planning. For instance, based on historical seasonal volume baselines on North American routes and early peak season signals identified in the current forecast, gradual fare increases are initiated two weeks in advance. This preemptive adjustment reduces the risk of customer attrition associated with abrupt fare hikes.

The dynamic adjustment strategy uses forecasted freight rate outputs as input. A multi-objective optimization model was constructed to achieve intelligent rate decision-making by integrating both operational constraints—such as capacity limits and minimum contract rates—and market competition objectives, including the retention of key customer segments and the pursuit of emerging market opportunities. Specifically, the forecasted rate fluctuation intervals were combined with node importance indicators to implement differentiated pricing strategies across customer groups. For core routes between hub ports, where sustained upward pricing pressure is forecasted over the next two weeks, a phased adjustment within contractual bounds is implemented to prevent cargo volume deflection caused by sudden rate increases. For non-core routes connecting feeder ports, if the dynamic graph detects temporary price-cutting by competitors, short-term supply–demand

elasticity predictions are used to preserve market share through price subsidies or bundled slot allocation strategies.

4 EXPERIMENT

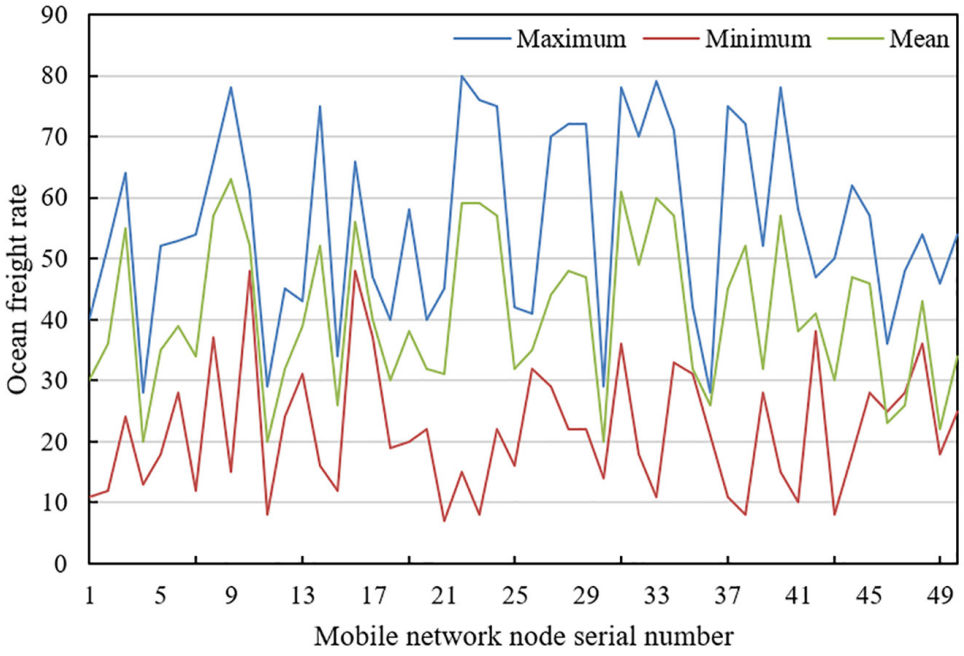

Fig. 4. Statistical distribution of predicted ocean freight rates for 50 mobile network nodes

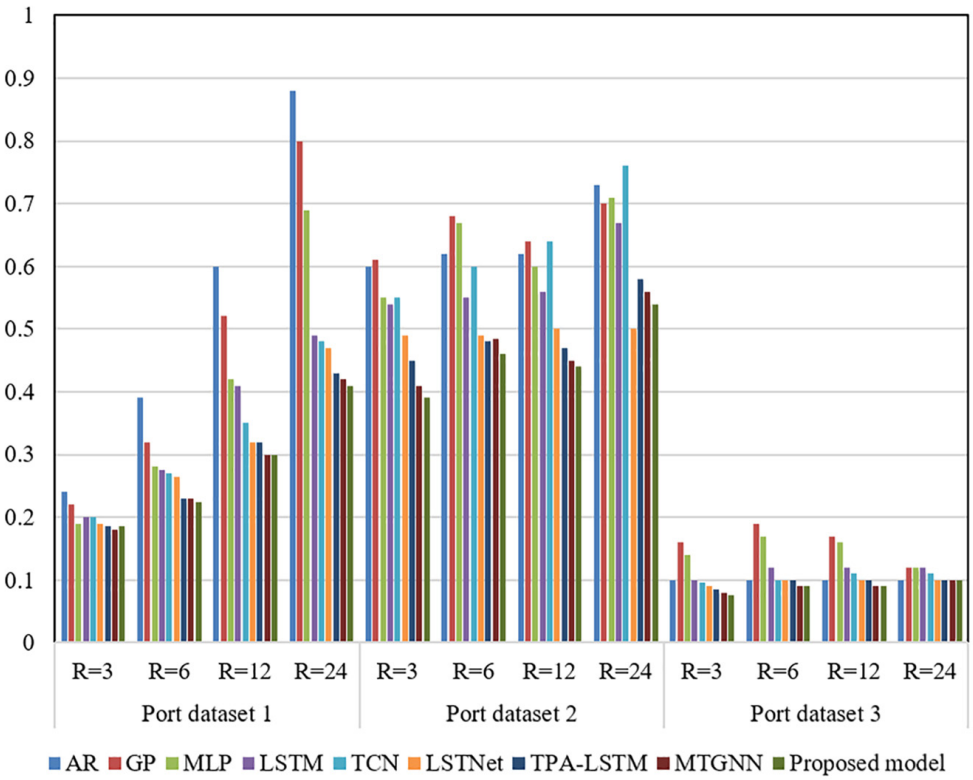

Fig. 5. RSE performance of different mobile ocean freight rate forecasting models at *R* time steps

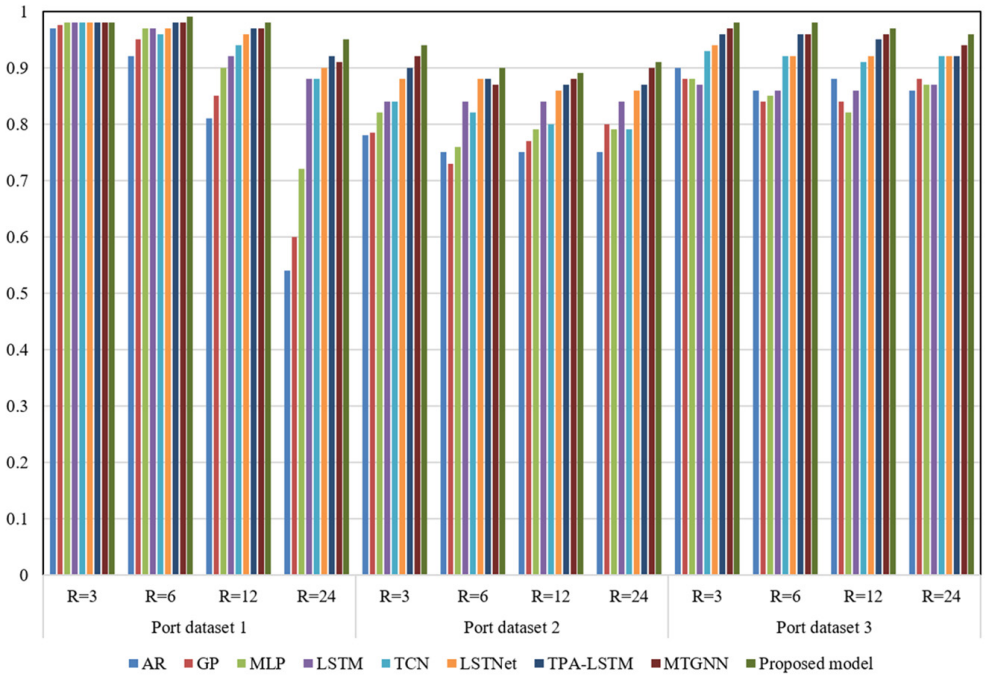

Fig. 6. CORR performance of different mobile ocean freight rate forecasting models at *R* time steps

Based on the statistical distribution of predicted ocean freight rates across 50 mobile network nodes illustrated in Figure 4, significant fluctuations and disparities are observed in the maximum (blue line), minimum (red line), and mean (green line) freight rates at each node. For instance, the maximum values at certain nodes reach elevated levels within specific intervals, indicating substantial volatility in freight rates at those locations. The mean value curve (green) also exhibits continuous oscillations, reflecting dynamic trends across different nodes. These variations and fluctuations highlight the inherently dynamic and time-varying nature of mobile ocean freight rates. Such patterns indicate that the freight rates of different nodes are strongly influenced by factors such as real-time supply and demand conditions and unexpected disruptions. This observation aligns with the previously established analysis of dynamic temporal characteristics. This further highlights the necessity of employing a GNN model based on multivariate time series, as proposed in this study, for ocean freight rate prediction. Such a model effectively captures both static structural features and dynamic temporal variations, enabling accurate forecasting and adaptive adjustments by automatically learning graph structure dependencies, thereby addressing the complex and fluctuating nature of ocean freight rates in real-world scenarios.

As illustrated in Figure 5, lower relative squared error (RSE) values indicate reduced prediction error. Across port datasets 1, 2, and 3, the proposed model consistently achieved lower RSE values compared to baseline models, including autoregressive model (AR), Gaussian process (GP), MLP, long short-term memory (LSTM), and temporal convolutional network (TCN), as the values of *R* changed. For instance, at *R* = 24 on port dataset 1, the proposed model yielded a significantly lower RSE than the comparison models. Turning to Figure 6, which reports CORR values, a higher score denotes stronger agreement between predicted and actual values. The proposed model maintained consistently high CORR values across all datasets and *R* values. Notably, at *R* = 12 on port dataset 2, a substantial improvement over several baseline models was observed. These results demonstrate that the proposed GNN model,

built upon multivariate time series and enhanced with a data-driven graph learning module, effectively captures both static structural features and dynamic temporal patterns. Compared with traditional models and other time-series models, by enabling deep fusion of static and dynamic graph structures, the proposed model achieves more accurate predictions of mobile ocean freight rates, reduces forecasting errors, and enhances the correlation between predicted and actual values. These results demonstrate the model's superiority in handling the complex characteristics of ocean freight rates and offer a more effective solution for data-driven, precise prediction and dynamic adjustment of mobile ocean freight rates.

As shown in Table 1 (50 time steps) and Table 2 (150 time steps), the proposed model consistently achieves lower mean squared error (MSE) and mean absolute error (MAE) values across port datasets 1, 2, and 3 when compared to baseline models such as convolutional LSTM (ConvLSTM), WaveNet, and deep temporal tensor factorization (DeepTTF). For example, in Table 1 for port dataset 1, the proposed model achieves an MSE of 0.342 and an MAE of 0.365, significantly outperforming ConvLSTM, which reports an MSE of 0.715 and an MAE of 0.668. Similarly, in Table 2 for port dataset 3, the proposed model achieves an MSE of 0.175 and an MAE of 0.265, clearly outperforming the comparison models. These results indicate that the proposed GNN model based on multivariate time series more effectively captures both the static structural features and dynamic temporal patterns in mobile ocean freight rate time series data. By integrating a data-driven graph learning module and an information interaction mechanism, the model delivers more accurate predictions. The lower MSE and MAE values across different time steps reflect reduced prediction errors, demonstrating the model's superiority over traditional and baseline models. This validates its effectiveness and advantage in precise prediction and dynamic adjustment of mobile ocean freight rates.

Table 1. Forecasting results for mobile ocean freight rates at 50 time steps

Model	Port Dataset 1		Port Dataset 2		Port Dataset 3	
	MSE	MAE	MSE	MAE	MSE	MAE
ConvLSTM	0.715	0.668	1.562	1.125	1.235	0.925
WaveNet	0.526	0.512	0.623	0.623	0.224	0.354
DeepTTF	0.748	0.748	1.784	1.112	0.516	0.579
Reformer	0.679	0.612	1.326	1.023	0.489	0.512
Autoformer	0.432	0.446	0.346	0.389	0.512	0.462
FedAvg	0.369	0.428	0.332	0.374	0.362	0.423
CausalGAN	0.358	0.379	0.248	0.332	0.145	0.258
Proposed model	0.342	0.365	0.239	0.327	0.312	0.315

Table 2. Forecasting results for mobile ocean freight rates at 150 time steps

Model	Port Dataset 1		Port Dataset 2		Port Dataset 3	
	MSE	MAE	MSE	MAE	MSE	MAE
ConvLSTM	1.145	0.854	4.213	1.568	1.235	0.925
WaveNet	0.689	0.623	2.365	1.124	0.241	0.356
DeepTTF	1.203	0.836	4.125	1.562	0.758	0.784

(Continued)

Table 2. Forecasting results for mobile ocean freight rates at 150 time steps *(Continued)*

Model	Port Dataset 1		Port Dataset 2		Port Dataset 3	
	MSE	MAE	MSE	MAE	MSE	MAE
Reformer	0.925	0.748	3.352	1.489	0.665	0.625
Autoformer	0.514	0.479	0.448	0.446	0.542	0.489
FedAvg	0.426	0.435	0.412	0.423	0.412	0.432
CausalGAN	0.487	0.489	0.512	0.512	0.189	0.289
Proposed model	0.426	0.425	0.336	0.378	0.175	0.265

As shown in Table 3, in port dataset 1, the absence of the graph learning module resulted in an RSE of 0.4215 and a CORR of 0.9152; without the graph interaction module, the RSE increased to 0.4458 with a CORR of 0.9126; and without MLP, an RSE of 0.4123 and a CORR of 0.9345 were recorded. The proposed model, by contrast, achieved an RSE of 0.4265 and a CORR of 0.9268. In port dataset 2, the configuration without the graph learning module yielded an RSE of 0.4758 and a CORR of 0.8452, while removing the graph interaction module produced an RSE of 0.4852 and a CORR of 0.8895. The exclusion of MLP resulted in an RSE of 0.4423 and a CORR of 0.8542. The proposed model achieved an RSE of 0.4326 and a CORR of 0.8796. In port dataset 3, the absence of the graph learning module and the interaction module led to RSEs of 0.1125 and 0.1145 and CORR values of 0.8895 and 0.8754, respectively. Excluding MLP resulted in a CORR of 0.9236 and an RSE of 0.1123. The proposed model achieved an RSE of 0.0956 and a CORR of 0.9254. These results indicate that each module plays a critical role in the model's predictive performance. The graph learning module enables the effective modeling of dependencies between static and dynamic graphs, while the graph interaction module facilitates their deep integration. MLP contributes significantly to the processing of features. The removal of any individual module led to noticeable degradation in performance, reflected by increased RSE values or diminished CORR values. By integrating these components, the proposed model consistently achieves lower RSE values and higher CORR values in most cases, demonstrating the necessity and synergistic effect of each module. These results underscore the importance of multi-component integration for accurate ocean freight rate prediction and further validate the rationality and effectiveness of the proposed multivariate time series GNN model.

Table 3. Ablation study results for mobile ocean freight rate forecasting

Model	Port Dataset 1		Port Dataset 2		Port Dataset 3	
	RSE	CORR	RSE	CORR	RSE	CORR
Without the graph learning module	0.4215	0.9152	0.4758	0.8452	0.1125	0.8895
Without the graph interaction module	0.4458	0.9126	0.4852	0.8895	0.1145	0.8754
Without MLP	0.4123	0.9345	0.4423	0.8542	0.1123	0.9236
Proposed model	0.4265	0.9268	0.4326	0.8796	0.0956	0.9254

5 CONCLUSION

This study addressed the problem of achieving accurate forecasting and dynamic adjustment of mobile ocean freight rates under a data-driven paradigm.

While significant value has been demonstrated, several limitations remain, pointing toward future research opportunities. From a methodological perspective, the study first provided an in-depth analysis of the data characteristics associated with mobile ocean freight rate forecasting. Static structural features and dynamic temporal patterns embedded in time series data were explored to provide foundational support for model development. Based on this, a GNN model tailored to multivariate time series was proposed. A data-driven graph learning module was employed to capture dependencies in both static and dynamic graphs, while a feature interaction mechanism was designed to enable their deep integration. This architecture addresses the subjectivity of manually defined graph structures and overcomes the limitations of single-graph modeling in conventional approaches. The proposed model exhibited superior performance across multiple evaluation metrics. In the comparative experiments, the proposed model achieved lower RSE and higher CORR, along with superior MSE and MAE values compared to baseline models such as ConvLSTM and WaveNet, demonstrating its capability to capture the complex characteristics of ocean freight rates and its high prediction accuracy. The ablation study confirmed the necessity of the synergy among the graph learning module, graph interaction module, and MLP. Training time analysis further revealed that the dynamic graph learning component improved training efficiency, enhancing the overall practicality of the model.

However, this study also has certain limitations. The model's complexity may be relatively high, which could constrain its applicability in scenarios with limited computational resources. Additionally, the scale and diversity of the datasets may be insufficient, with limited coverage of highly complex scenarios. The ability to capture certain dynamic features also remains open to further improvement. Future research may explore several directions: (a) optimizing the model architecture to reduce computational costs and enhance efficiency; (b) expanding the dataset size and enriching scenario types to enhance the model's generalization ability; (c) incorporating more external factors to deepen the dynamic adjustment strategy; and (d) exploring the model's application in real-time freight rate adjustments to enable more precise dynamic responses. These directions aim to further refine the model, enhance its practicality and adaptability, and provide more robust decision support for the maritime shipping industry.

6 REFERENCES

[1] G. Mundaca, J. Strand, and I. R. Young, "Carbon pricing of international transport fuels: Impacts on carbon emissions and trade activity," *Journal of Environmental Economics and Management*, vol. 110, pp. 102517, 2021. https://doi.org/10.1016/j.jeem.2021.102517

[2] A. H. Becker *et al.*, "A note on climate change adaptation for seaports: A challenge for global ports, a challenge for global society," *Climatic Change*, vol. 120, pp. 683–695, 2013. https://doi.org/10.1007/s10584-013-0843-z

[3] A. M. Goulielmos and P. Plomaritou, "A review of marketing for tramp shipping," *International Journal of Shipping and Transport Logistics*, vol. 1, no. 2, pp. 119–155, 2009. https://doi.org/10.1504/IJSTL.2009.024492

[4] E. Bulut, O. Duru, and S. Yoshida, "Market entry, asset returns, and irrational exuberance: Asset management anomalies in dry cargo shipping," *International Journal of Shipping and Transport Logistics*, vol. 5, no. 6, pp. 652–667, 2013. https://doi.org/10.1504/IJSTL.2013.056851

[5] M. Fusillo, "The stability of market shares in liner shipping," *Review of Industrial Organization*, vol. 42, pp. 85–106, 2013. https://doi.org/10.1007/s11151-012-9359-3

[6] R. Adland, F. E. Benth, and S. Koekebakker, "Multivariate modeling and analysis of regional ocean freight rates," *Transportation Research Part E: Logistics and Transportation Review*, vol. 113, pp. 194–221, 2018. https://doi.org/10.1016/j.tre.2017.10.014

[7] J. Chi, "Exchange rate and transport cost sensitivities of bilateral freight flows between the US and China," *Transportation Research Part A: Policy and Practice*, vol. 89, pp. 1–13, 2016. https://doi.org/10.1016/j.tra.2016.05.004

[8] M. Aydos, Y. Vural, and A. Tekerek, "Assessing risks and threats with layered approach to Internet of Things security," *Measurement and Control*, vol. 52, nos. 5–6, pp. 338–353, 2019. https://doi.org/10.1177/0020294019837991

[9] A. Talib, M. Housni, and M. Radid, "Utilizing M-technologies for AI-driven career guidance in Morocco: An innovative mobile approach," *International Journal of Interactive Mobile Technologies*, vol. 17, no. 24, pp. 173–188, 2024. https://doi.org/10.3991/ijim.v17i24.44263

[10] J. Zheng, X. Wang, and K. Zhou, "Empirical test on the relationship between financial region ecological environment and enterprise risk taking based on OLS regression model," *Ekoloji Dergisi*, vol. 27, no. 106, pp. 1809–1818, 2018.

[11] Z. Tan, Q. Meng, F. Wang, and H. B. Kuang, "Strategic integration of the inland port and shipping service for the ocean carrier," *Transportation Research Part E: Logistics and Transportation Review*, vol. 110, pp. 90–109, 2018. https://doi.org/10.1016/j.tre.2017.12.010

[12] A. Harrison and J. Fichtinger, "Managing variability in ocean shipping," *The International Journal of Logistics Management*, vol. 24, no. 1, pp. 7–21, 2013. https://doi.org/10.1108/IJLM-05-2013-0052

[13] S. N. Singh and A. Mohapatra, "Repeated wavelet transform based ARIMA model for very short-term wind speed forecasting," *Renewable Energy*, vol. 136, pp. 758–768, 2019. https://doi.org/10.1016/j.renene.2019.01.031

[14] S. Ray, A. Lama, P. Mishra, T. Biswas, S. S. Das, and B. Gurung, "An ARIMA-LSTM model for predicting volatile agricultural price series with random forest technique," *Applied Soft Computing*, vol. 149, pp. 110939, 2023. https://doi.org/10.1016/j.asoc.2023.110939

[15] W. Huang *et al.*, "Railway dangerous goods transportation system risk identification: Comparisons among SVM, PSO-SVM, GA-SVM and GS-SVM," *Applied Soft Computing*, vol. 109, pp. 107541, 2021. https://doi.org/10.1016/j.asoc.2021.107541

[16] V. K. Chauhan, K. Dahiya, and A. Sharma, "Problem formulations and solvers in linear SVM: A review," *Artificial Intelligence Review*, vol. 52, pp. 803–855, 2019. https://doi.org/10.1007/s10462-018-9614-6

[17] Z. Zhang, J. Leng, L. Ma, Y. Miao, C. Li, and M. Guo, "Architectural implications of graph neural networks," *IEEE Computer Architecture Letters*, vol. 19, no. 1, pp. 59–62, 2020. https://doi.org/10.1109/LCA.2020.2988991

[18] A. J. Fofanah, D. Chen, L. Wen, and S. Zhang, "Addressing imbalance in graph datasets: Introducing gate-gnn with graph ensemble weight attention and transfer learning for enhanced node classification," *Expert Systems with Applications*, vol. 255, pp. 124602, 2024. https://doi.org/10.1016/j.eswa.2024.124602

7 AUTHOR

Xinning Kang was born in Ganzhou, Jiangxi, China, in 2004. Currently, she works in Shanghai Maritime University (E-mail: xinningkang2004@163.com).